SIMILARITIES BETWEEN ATOMIC PROPERTIES IN DENSE AND OPEN ALUMINOPHOSPHATE SIEVES

Larin, A.V.[1,2], Porcher, F.[3], Aubert, E.[3], Souhassou, M.[3] and Vercauteren, D.P.[1]

[1]Laboratoire de Physico-Chimie Informatique, Université de Namur, B-5000 Namur, Belgium.
E-mail: daniel.vercauteren@fundp.ac.be
[2]Department of Chemistry, Lomonosov MSU, Moscow, B-234, 119899, Russia. [3]Laboratoire de Cristallographie et Modélisation des Matériaux Minéraux et Biologiques (LCM[3]B), CNRS UMR 7036, Université Henri Poincaré Nancy I, B.P. 239, F-54506 Vandœuvre-lès-Nancy, France.

ABSTRACT

Experimental studies on the $AlPO_4$-15 sieve are combined with theoretical analyses of the charge partitioning between the sieves and different (water, ammonium, *i*-propylamine) template molecules (TM) to ascertain the ionic character of the interactions occurring between the different partners. Positions of the TM protons are optimized using *ab initio* periodic Hartree-Fock calculations under fixed positions of the non-hydrogen atoms obtained by XRD. The critical points of the X_{temp}-H…O_{sieve} (X = N, O) hydrogen bonds as well as of the Al-O bonds of the experimental electron density are compared to the ones computed at different theory levels.

INTRODUCTION

The large diversity of aluminophosphates (ALPOs) [1], their high thermoresistivity [2], and the possibility to incorporate elements with a higher coordination number than 4 have made the ALPOs attractive models for the synthesis of various classes of molecular sieves. Promising types are the MeAPO sieves (i) including a Me metal such as Co, Ni ..., in the framework (ii) cationic forms or (iii) hydrogen forms which are obtained *via* partial replacement of the P atoms by Si (SAPOs) whose lower charge is compensated by cations or protons. Additionally, when containing template molecules (TMC), these sieves represent an intermediate form before calcination and may include elements which are not found in the calcined forms such as the AlO_5, AlO_6, and $HOAl_3$ groups.

So far, the understanding of the mechanism for the ALPOs formation has been grounded exclusively on empirical data. For example, the protonation of the *i*-propylamine template is proposed in $AlPO_4$-14 (AFN type) [3]. The absence of theoretical data is related, on one side, on the essential role of the liquid phase whose simulation is rather complicated. Despite the important role of hydrates and the consideration of hydrogen bonding (HB) into molecular modeling of zeolite synthesis [4], the role of HB for these sieves has not yet been clearly discussed. Particularly, the competition between $OAlO_3$ and H_2O to form HB with the template protons can be of crucial role for the growth of the sieves. On the other side, the ionic character for ALPOs as compared to SiO_2-based or aluminosilicate zeolites presents a serious problem for calculations with both the cluster approach [5-6] and the embedded QM/MM scheme. Hence, MeAPOs [7], SAPOs [8-10], and ALPOs [7, 11-12] are particularly interesting materials that need to be tackled using periodic calculations *via* either AIMD [8-9], periodic Hartree-Fock (PHF) [13], or empirical force fields with, for example, the GULP code [14]. The possibility to construct approximate functions for high order atomic multipole moments (AMMs) for "small size" calcined ALPOs was already shown in order to solve the electrostatic aspects in QM/MM modeling of these systems [11]. Moreover, the application of methods keeping periodic conditions to the TMC sieves could provide new information about their properties considering the particular sieve fragments already mentioned whose stability determines their facility of transformation during calcination. To our knowledge, neither the Al properties for the various AlO_n configurations, nor the X_{temp}-H…O_{sieve} (X = N, O) hydrogen bonds have not yet been characterized theoretically in ALPOs containing TMs at the PHF or periodic DFT (PDFT) level. A clarification of the nature of the interactions in ALPO - template complexes could thus clearly help to guide the experimental conditions required for their synthesis as well as for accurate molecular modeling.

In this paper, we combine theoretical studies of as-synthesized $AlPO_4$-14 and $AlPO_4$-15 sieves and X-ray diffraction (XRD) results for $AlPO_4$-15. Particularly, we present theoretical characterizations of two TMC

Proceedings: 14th International Zeolite Conference
Editors: E. van Steen et al
ISBN: 0-958-46636-X
25 – 30 April 2004
Cape Town, South Africa
Produced by: Document Transformation Technologies

sieves including water ($AlPO_4$-14 and $AlPO_4$-15), ammonium ($AlPO_4$-15), and *i*-propylamine ($AlPO_4$-14). In the first part, partial optimizations of the XRD models of the TMC sieves are realized for the protons participating in the HB between the template and the framework. Then, charge partitionings between the sieve and the TMs are evaluated with single point PHF calculations. In the second part, we compare the calculated and experimental electron densities (EDs) at the bond critical points (CPs) for both as-synthesized forms. AMMs of the different crystallographic atom types for open and dense forms of the calcined and both TMC sieves are compared.

COMPUTATIONAL DETAILS AND EXPERIMENTAL PART

All calcined ALPO forms were optimized with the Catlow force field (FF) [15, 16] using GULP [14]. The X-H distances (X = N, O) of the templates were optimized with the *ab initio* PHF CRYSTAL98 code [13]. In order to calculate the electronic properties, *i.e.*, charge distributions, ED, density of states, …, of the $AlPO_4$-14 [3], $AlPO_4$-15, and calcined sieves (Table 1), single point calculations were performed at the split valence plus polarization functions mentioned below as 6-21G** level with PHF as well as with PDFT using the B3LYP and Perdew-Burke-Ernzerhof (PBE) functionals. Minor variations for the exponents of the Al, O, H, and P atoms between the TMC forms were needed to achieve SCF convergence. All charge evaluations with CRYSTAL have been done with the Mulliken scheme, the only available in this code. The search and characterization of all the bond CPs (*i.e.*, the saddle points along the bonds) were performed, within Bader's AIM theory [20], with TOPOND96 [21] for the calculated EDs and with NEWPROP [22] for the experimental ED. For comparison, charge evaluations of the template molecule in the free state were also done with GAUSSIAN98 [23] with the same basis set as used for the PHF calculations.

Single crystals of $AlPO_4$-15 ($NH_4Al_2(OH)(H_2O)(PO_4)_2{\cdot}H_2O$) ($P2_1/n$, a = 9.556 Å, b = 9.563 Å, c = 9.615 Å, β = 103.58°) were obtained by hydrothermal synthesis (180°C); the XRD data were collected at 115 K on a Nonius K CCD diffractometer using Mo(Kα) radiation. The charge density was modelled according to the multipolar formalism of Hansen and Coppens (MoPro software). The final residual indices are R = 1.02%, Rw = 0.66%, N_{obs} = 4725, N_{par} = 510, $(\sin\theta/\lambda)_{max}$ = 0.90 $Å^{-1}$ [19].

Table 1. Symbols, number of atoms per unit cell (UC), of different Al, P ($n_P = n_{Al}$), and O types ($n_N = 1$), of atomic orbitals (AO) per UC, and symmetry group of the aluminophosphate sieves[a], all of them corresponding to the Al/P = 1.

Name	Symbol	Atoms/UC	n_{Al}/n_O	AO/UC (6-21G**)	Symmetry group
$AlPO_4$-14 (as-synth.)[b]	AFN	86	4/18	1034	$P\bar{1}$
$AlPO_4$-15 (as-synth.)[c]	-	100	2/11	1140	$P2_1n$
$AlPO_4$-41	AFO	60	4/13	920	$Cmc2_1$
$AlPO_4$-18	AEI	72	3/12	1040	C2/c
$AlPO_4$-5	AFI	72	1/4	1104	P6cc
$AlPO_4$-H2	AHT	36	2/7	552	$Cmc2_1$
$AlPO_4$-31	ATO	36	1/4	552	R3
MeAPO-39	ATN	24	1/4	432	I4
Berlinite[d]	-	18	1/4	276	$P3_121$

[a] coordinates from ref. [17]; [b] coordinates from ref. [18], n_H = 13; [c] coordinates from ref. [19], n_H = 9; [d] ref. [19]

GEOMETRY OPTIMIZATIONS

$AlPO_4$-14 sieve

The coordinates of the $AlPO_4$-14 TMC sieve were kindly given by R.W. Broach [18], who corrected some H positions as compared to within the first published structure [3]. Because all C-H and N-H bonds of *i*-propylamine were strongly shortened as compared to standard values, the bond lengths were varied for all H which could be concerned by HB. Coordinates of all non-hydrogen atoms were fixed as in the XRD model. The C-H and N-H values were increased based on values calculated for the isolated protonated template ion with GAUSSIAN98 (|N-H| = 1.0152 and 1.0159 Å, $|C\text{-}H_C|$ is between 1.089 and 1.092 Å for all hydrogens H_C linked to C atoms). Such approximation for the $|C\text{-}H_C|$ distance is justified by long $H_C\ldots O_{sieve}$ distances for all H_C and is confirmed by the Mulliken charges on the template atoms calculated with CRYSTAL98 or GAUSSIAN98 (Table 2).

Table 2. Mulliken atomic charges on the i-propylamine template in $AlPO_4$-14 calculated with CRYSTAL98 (A), the isolated *i*-propylamine ion (B, C), and the neutral form (D), the two last ones being optimized with GAUSSIAN98 using the HF/6-21G** (A, B, D) and B3LYP/cc-pVTZ (C) levels.

Atoms	A	B	C	D
N 1	-0.3812	-0.4342	0.0477	-0.5790
C 2	0.2566	0.2529	-0.0625	0.3010
C 3	0.0074	-0.0066	-0.2707	0.0344
C 4	0.0026	-0.0066	-0.2707	0.0240
H 5	*0.2303*	*0.3051*	*0.2007*	*0.1765*
H 6	*0.2214*	*0.3051*	*0.2007*	*0.1736*
H 7	*0.2102*	*0.3022*	*0.1950*	-
H 8	-0.0079	0.0248	0.1248	-0.0027
H 9	-0.0003	0.0248	0.1248	-0.0274
H 10	0.0048	0.0597	0.1460	-0.0199
H 11	-0.0114	0.0248	0.1241	-0.0252
H 12	0.0043	0.0248	0.1248	-0.0242
H 13	0.0102	0.0597	0.1460	-0.0173
H 14	0.0114	0.0635	0.1698	-0.0157
Total	0.5380	1.0000	1.0000	0.0000

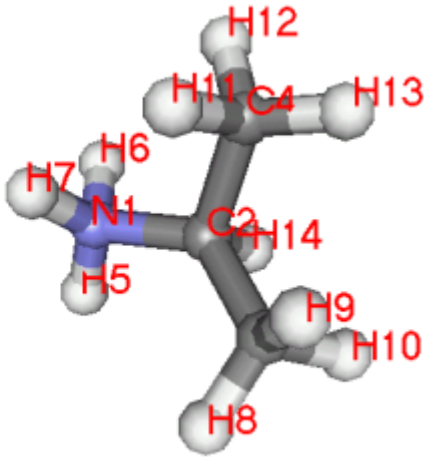

In order to quantitatively estimate the accuracy of the HB geometry computed with PHF, we evaluated the correlation between the elongations ΔR_{X-H} of the valence X-H bonds (X = N, O) with respect to the ones of the isolated gas state species *versus* the HB length (Figure 1). Respective data were already published for the O-H bond in $(H_2O)_n$ clusters at the HF and MP2 levels with accurate correlated basis sets [24] (diamonds in Figure 1). We note that if the absolute O-H lengths depend on the theoretical level/basis set, the $\Delta R_{X-H} = R_{X-H} - R^g_{X-H}$ elongations owing to HB relative to the bond length R^g_{X-H} in the gas (g) state are less sensitive to these factors and are close for HF and MP2.

Question of the N-H bonds, absolute N-H lengths were measured experimentally, *i.e.*, including anharmonic increase, as 1.03 Å [25], and calculated values of 1.007-1.053 Å and 1.01- 1.03 Å were obtained for aluminosilicates with embedded [26] and PHF [27] approaches. For the ions, respective gas state N-H bond lengths R^g_{N-H} were evaluated with GAUSSIAN98 as 1.0174 and 1.0088 Å for NH_4^+ and *i*-$C_3H_7NH_3^+$, respectively, to serve as landmarks. The last R^g_{N-H} is a mean value between the asymmetric bonds of 1.0095 and 1.0081 Å in the neutral form. (We have chosen the neutral molecule and not the cation for comparison of the N-H elongation in the TM because the distance C-N of 1.478 Å obtained with PHF/6-21G** level is much closer to 1.463 Å in the neutral TM. This distance is particularly sensitive to the protonation as shown below.) The comparison shows that the absolute N-H bond lengths in the gas state are shorter in *i*-$C_3H_7NH_3^+$ than in NH_4^+ and their relation after considering HB elongations is not due to shorter HB of the H atoms, *i.e.*, 1.0136, 1.0142, 1.0154 Å in *i*-$C_3H_7NH_3^+$ and 1.0170, 1.0260, 1.0292, 1.0303 Å in NH_4^+. The HF optimization of the H_2O geometry with 6-21G** resulted in O-H = 0.9551 Å and H-O-H = 99.91°, which is much smaller than the experimental H-O-H value of 103.9° [28]. Because the underestimated H-O-H angle leads to a longer O-H bond, the O-H length of H_2O was also optimized at fixed experimental 103.9° angle, which yielded R^g_{O-H} = 0.9531 Å, the length used for the evaluation of the O-H elongations (Figure 1).

Protonation is crucial for the geometry of *i*-$C_3H_7NH_2$. If the increase of the N-H distances is small upon protonation for NH_3, 0.0066 Å, and *i*-$C_3H_7NH_2$, 0.0089 Å, the C_2-N length in *i*-$C_3H_7NH_3^+$ drastically increases from 1.463 to 1.550 Å at the HF/6-21G** level. These values vary slightly with the method, 1.469 and 1.541 Å with MP2/6-21G**, but more seriously with the method/basis set, 1.468 and 1.528 Å with MP2/6-311+G**. The most visible change in the TM skeleton is related with the appearance of a symmetry plane upon protonation (see equivalence of the charges of primary C_3 and C_4, Table 2) so that the two C-C bonds become equal to 2.479 Å instead of 2.426 and 2.502 Å in the free molecule. This ion/molecule difference is held at all higher theory levels used.

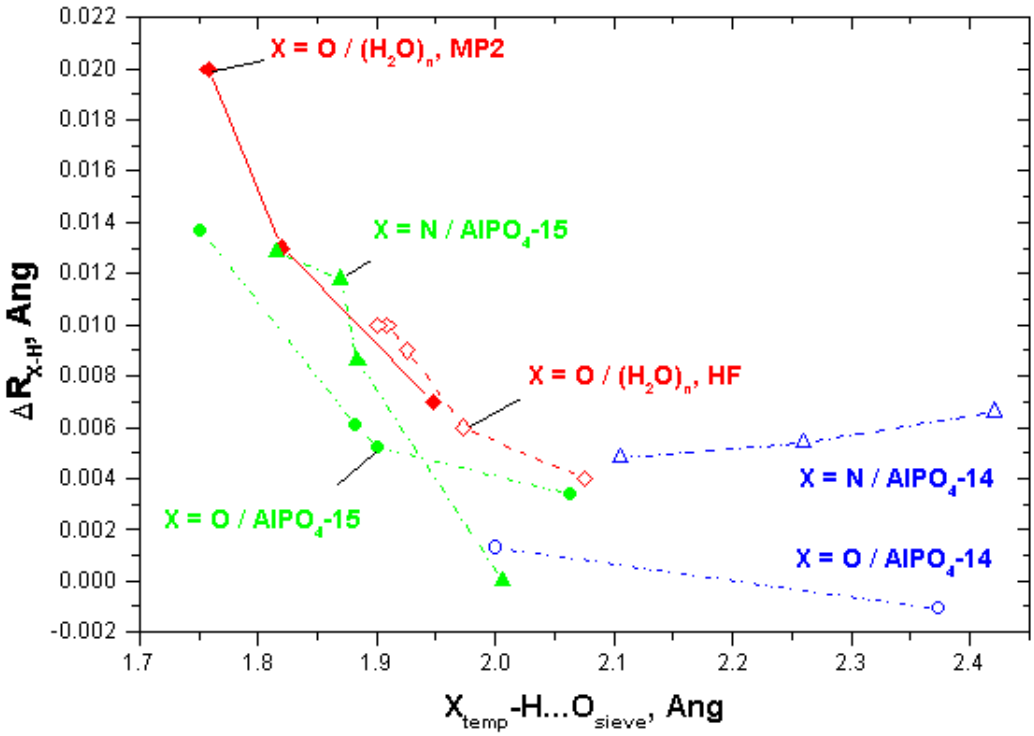

Figure 1. Correlation between the increase ($\Delta R_{X\text{-}H}$, Å) of the X-H bond length (X = N, O) with respect to the gas state value *versus* the X_{temp}-H…O_{sieve} hydrogen bond length (Å) for H_2O (circles), ammonium ion (triangles), and *i*-propylamine ion (triangles) included in $AlPO_4$-14 (open symbols) and $AlPO_4$-15 (closed symbols). Correlation $\Delta R_{O\text{-}H}$/O…H is also given for $(H_2O)_n$ clusters at the HF (n = 2 - 6, open diamonds) and MP2 (n = 2 - 4, closed diamonds) levels both with the aug-cc-pVDZ basis set [24].

$AlPO_4$-15 sieve

The XRD model of the $AlPO_4$-15 sieve includes two H_2O molecules and NH_4^+ [19]. NH_4^+ conserves a nearly tetrahedral configuration with H-N-H angles ranging between 104°5 and 114°1 and nearly equal |N-H| bonds of 0.9981, 0.9981, 0.9984, and 0.9987 Å. Taking into account the variety of relatively short HB of 1.82, 1.87, 1.88, 2.01 Å between the hydrogens of NH_4^+ and the oxygens of the $AlPO_4$-15 framework, we admitted a higher variation between the N-H lengths as compared to the ones shown by XRD. Indeed, a smaller size for NH_4^+ allows closer contacts with the ALPO oxygens and thus a more effective HB scheme. Elongations of N-H in NH_4^+ are larger than in *i*-$C_3H_7NH_3^+$ and occasionally coincide with the O-H dependence with the O_w…H_w length as calculated at higher theory level (diamonds in Figure 1) [24].

A $(H_2O)_2$ dimer with a shortened O…O distance of 2.701 Å as compared to the one in the isolated dimer, *i.e.*, near 2.90 Å [24], has been observed in $AlPO_4$-15. More precisely, one H_2O proton is hydrogen bonded with a value of 1.758 Å to the O of the neighbor molecule while all other three Hs are hydrogen bonded to the O atoms of the sieve. This geometry does not coincide to the one calculated in the gas state [24]; accurate PHF optimizations of the H_2O position could thus be helpful. This experimental evidence of the presence of $(H_2O)_2$ in $AlPO_4$-15 is important for the modeling of zeolite or sieve synthesis wherein H_2O monomers usually serve as building units [29].

Comparison of the HBs in the $AlPO_4$-14 and $AlPO_4$-15 sieves

The slight increase of the N-H bond lengths in *i*-$C_3H_7NH_3^+$ observed *versus* the wide X_{temp}-H…O_{sieve} distance, changing from 2.1 to 2.4 Å (open triangles in Figure 1), is contrary to the predicted N-H shortening if a N-H/O…H correlation exists as for $AlPO_4$-15 (closed triangles in Figure 1). No large influence due to HB on the *i*-$C_3H_7NH_3^+$ geometry in $AlPO_4$-14 was observed. If the TM geometry is not controlled by HB, then one suggests that such conclusion is also justified for the total interaction between the TM and the sieve. It means that *i*-$C_3H_7NH_3^+$ remains attached to the framework mainly because of electrostatic interactions. Evidently, this can be the result of a TM motion from the favored position during the ALPO formation; however, such hypothesis does not look as reliable owing to the N position relative to the sieve oxygens at distances of 2.88, 3.24, 3.38, and 3.86 Å. The three first values are not far from those for the H_2O oxygens in the hydration sphere of the amino-group [29]. Moreover, the O_{sieve} atom closest to N possesses the largest charge (-0.466 e^-)

through all O types of the sieve. The remote position of H_2O relative to the TM confirms that the TM does not hold its hydration sphere and is hindered sterically to create HB with H_2O within the pores.

CHARGE DISTRIBUTION AND ELECTRON DENSITY

Charge distributions

Periodic calculations with PHF and B3LYP for the corrected $AlPO_4$-14 XRD structure led to the total charge of +0.538 e^- (Table 2) and to +0.326 e^- for *i*-$C_3H_7NH_3^+$, respectively. So, the usual hypothesis on the ionic form of the alkyl amino-template is supported in a different extent at both levels of theory. These values can be compared with the smaller charges of +0.323, +0.194, and +0.224 e^- for NH_4^+ in $AlPO_4$-15, as calculated with PHF, and B3LYP and PBE functionals, respectively. The charges corresponding to the 6-21G** basis set are the lowest ones with respect to the ones obtained with other basis sets applied for calcined forms [7] whose ionicities should sharply increase at other basis set levels. Hence, one can predict only increase of the charges with other bases. For comparison of the charge distributions induced by the framework, the isolated *i*-$C_3H_7NH_3^+$ and NH_4^+ ions, as well as the *i*-$C_3H_7NH_2$ molecule were optimized with the same basis set as applied with PHF. The dipole character of the charge distribution between the secondary carbon C_2 and the N atom in both the *i*-propylamine cation and molecule is not proved at the highest MP2/6-311+G** and B3LYP/cc-pVTZ levels (Table 2). In the MP2/6-311+G** case, *i*-$C_3H_7NH_3^+$ corresponds to a "polarized" form between the C, N, on the one side, and the H atoms, on the other, shifting the large positive charge of +0.724 e^- towards NH_3 and much smaller ones to the methyl groups, +0.126 e^- per CH_3. This 3-site charge distribution includes a nearly neutral CH group, +0.024 e^-; it does not coincide neither to the dipolar type, nor to the absolute charges obtained with B3LYP/cc-pVTZ so that a verification with a more accurate theory level is recommended. The obtained charges can however give an idea of the field strength influencing the H_2O molecules forming the hydration sphere around the amino-group.

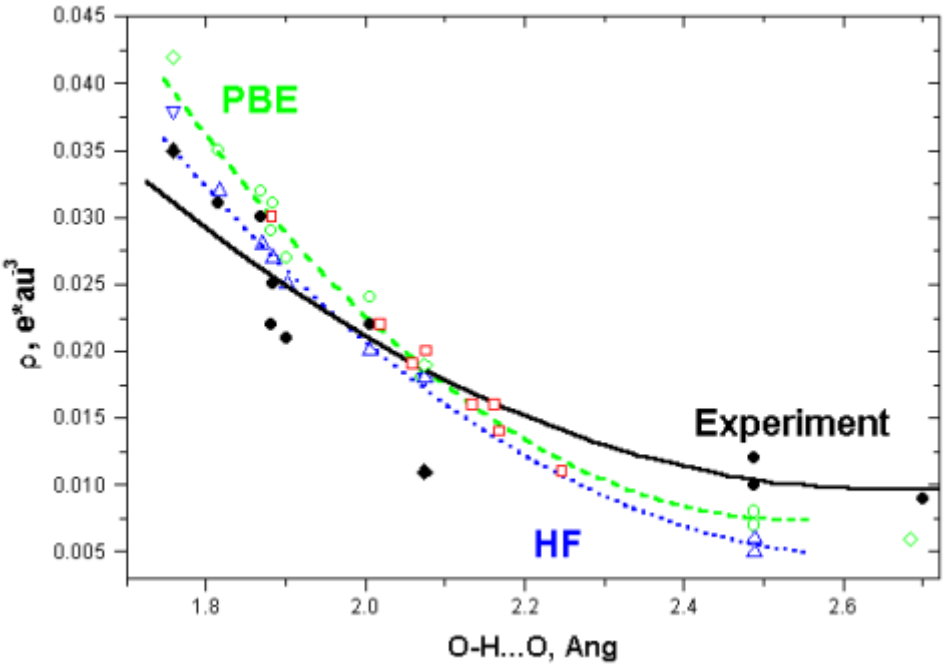

Figure 2. Experimental (closed symbols) and 6-21G** calculated (open symbols) electron density at the CP positions of the H O hydrogen bonds in $AlPO_4$-15. Experimental values are shown for HB to the framework O_f (circles) and H_2O O_w (diamonds) oxygen atoms; PDFT values, by diamonds and circles for the O_f and O_w oxygens, respectively; PHF values, up triangles for the O_f and down triangles for O_w oxygens, respectively. Quadratic approximations are shown for the experimental values (solid line) as well for the ones calculated with PDFT (dashed line) and PHF (dotted line). PBE/ps-21G** ED calculated values for H_2O adsorbed in two small size aluminosilicates are shown by squares [30].

Comparison of the ED at the bond CP positions of the H…O and Al-O bond types

An important part of work consisted in the comparison of the characteristics of the bond CPs obtained from the analysis of the experimental ED (ρ), using NEWPROP, with the respective parameters of the CPs obtained with TOPOND from the calculated ED. Looking to all CPs of the HBs (Figure 2), one notes that the

calculated ED of $AlPO_4$-15 is overestimated for short O_{temp}-H…O distances and underestimated at longer ones with both PDFT and PHF methods, while the slope of the PHF calculated ED *versus* O_{temp}-H…O looks closer to the experimental one.

As mentioned earlier, the as-synthesized forms present different AlO_n configurations. All of them, n = 4, 5, 6, occur in $AlPO_4$-14 whereas AlO_6 is only present in $AlPO_4$-15. The coordination number seems not to influence the Al donor character in the Al-O bonds. It is evidenced by the linear approximation of the experimental ED at the CP(Al-O) positions *versus* the Al-O distance. These experimental ρ(Al-O) ED data, including the AlO_4 type of berlinite [19] and the AlO_6 type of $AlPO_4$-15 [19], are described by a linear fit (r^2 = 0.99) (results are omitted for shortness). Additionally, the similarity between the highest occupied states of Al in the different AlO_n types is confirmed by the similar densities of states obtained for all types of Al coordination (n = 4 – 6) appearing in $AlPO_4$-14.

Multipolar representation of the ED in the TMC and calcined ALPOs

In ref. [11], we showed that the electrostatic potential in the internal space available for adsorbed species in ALPOs is mainly determined by the octupole MMs at the different crystallographic types of Al and P atoms as well as the dipole and quadrupole MMs at the oxygens. Hence, the search of approximate dependences for these moments at least is required as well as for the additional atom types which are important in the TMC sieves because of their possible interactions with the nearest neighbors. Five- and six-coordinated AlO_n are typical of the TMC sieves. For O atoms, two distinctions of O including bonds in the TMC sieves as compared to the calcined ones could be added: (1) Al-O bonds which are elongated up to 1.90 Å for the octahedral Al and (2) the presence of HB oxygen atoms. First, as performed in [11], we obtained an accurate approximation in terms of "cumulative coordinate" (CC) of the Al hexadecapole at the AlO_n positions with a correlation of r^2 = 0.94 including all Al types (n = 4 – 6) in both TMC sieves (Figure 3a). Second, we applied separate approximations of the AMMs for the three O types (two of them are shown by lines in Figure 3b). No difference between the AMMs of the oxygens in the calcined ALPOs and the ones in the TMC sieves participating in the long Al-O bonds at the level of the dipolar moments is observed (Figure 3b). However, the Al-O increase has a different influence on the AMMs of different orders for the oxygens. Generally, an Al-O increase lowers the accuracy of the CC approximation. As it was shown earlier [12], the longer Al-O and the larger difference between the Al-O and P-O bond lengths should increase the total O dipole which is in agreement with the observed trend. We did not observe any difference between the $AlPO_4$-14 ("open" form) and $AlPO_4$-15 ("dense" form) sieves even though the comparison of only two TMC forms is not sufficient to ascertain it totally. Additionally, we noted the existence of a clear difference between the O types as, for example, between the HB oxygens and the ones which do not participate in HB. Participation in HB (closed symbols in Figure 3b) leads to a worse CC approximation of the oxygen AMMs. Let us mention that the preliminary geometry optimization with the Catlow FF [15-16] of the calcined ALPOs allowed to improve the accuracy of the approximation for all AMMs.

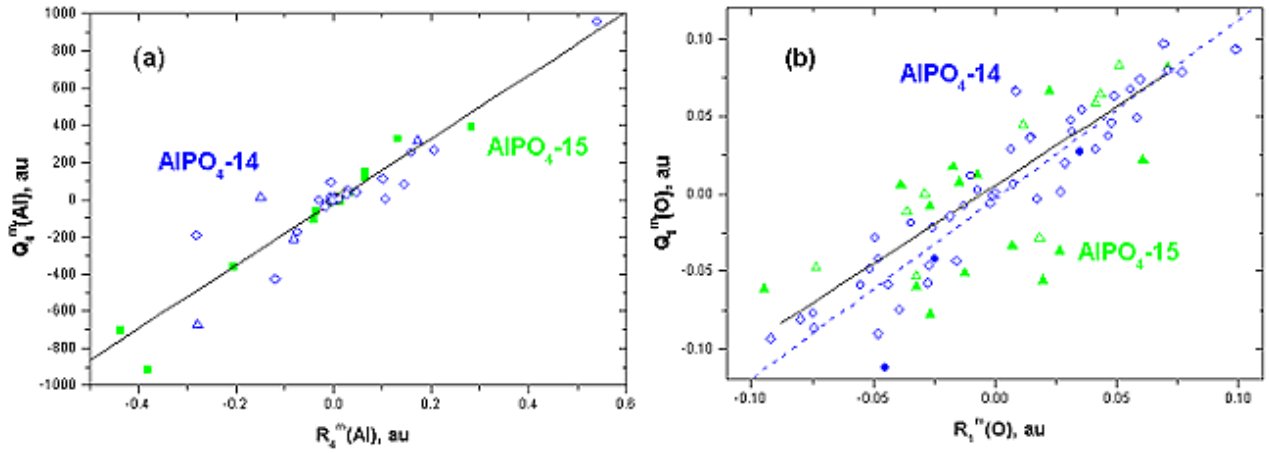

Figure 3. Dependence *versus* the "cumulative" $R_L^m(X)$ coordinate of the (a) hexadecapole $Q_4^m(Al)$, |m| = 0-4, and (b) dipole $Q_1^m(O)$, |m| = 0-1, calculated at the PHF/6-21G** level for $AlPO_4$-14 (open symbols in a, circles and diamonds in b) and $AlPO_4$-15 (closed symbols in a, triangles in b). A common analytical approximation is presented in (a) and separate approximations in (b) for O atoms with elongated Al-O bonds (dashed line) and for the O atoms not participating in the HBs (solid line). AMMs are shown for HB oxygen atoms (closed symbols), for non-HB oxygen atoms (open symbols), and the O atoms participating in the elongated Al-O bonds (diamonds).

It is also important to consider the density *d* of the frameworks for the two considered TMC sieves as it gives an implicit information about the available internal volume. $AlPO_4$-15 does not exist in calcined form due to decomposition after the loss of the second H_2O molecule [31]. Its density should be sufficiently large, while the calcined AFN *d* value is 17.4 T/1000 $Å^3$, an intermediate value for the ALPOs family. In order to evaluate the variation of the parameters of the approximations of the AMMs between the various calcined ALPOs, different approximations were considered for two separate sets of ALPOs classified according to their framework densities: $18.4 > d \geq 14.5$ T/1000 $Å^3$, *i.e.*, AEI, AFI, AFN, ATN ("open" models), and $d \geq 18.4$ T/1000 $Å^3$, *i.e.*, AHT, AFO, ATO, and berlinite ("dense" models). Approximations of the same high quality as shown in [11] for the AMMs coincide for both two groups of calcined ALPOs. The large number of calcined ALPOs considered allows thus to conclude on the absence of systematic variation between the dense and open ALPOs.

CONCLUSIONS

Experimental and theoretical studies were combined to characterize the structural and electronic features of a series of ALPO sieves with and without template molecules. The positions of the H atoms in $AlPO_4$-14 and $AlPO_4$-15 as well as of the template (water, ammonium, *i*-propylamine) atoms were optimized with the *ab initio* periodic Hartree-Fock (PHF) CRYSTAL98 code under fixed positions of the non-hydrogen atoms. The charge partitioning between the sieve and template proved the ionic character of the protonated *I*-$C_3H_7NH_3^+$ template. No confirmation of the role of the hydrogen bonds (HB) was observed for *i*-$C_3H_7NH_2$ in $AlPO_4$-14. On the contrary, correlations between the N_{temp}-H/H…O_{sieve} distances proved that the NH_4^+ geometry in $AlPO_4$-15 is controlled by the HBs. It is possible that this difference between the HBs in $AlPO_4$-15 and $AlPO_4$-15 is the result of different densities of the two sieves. In the denser $AlPO_4$-15, small molecules can be trapped or be templates forming relatively short HB lengths. In the open sieves, the interaction energy terms depending on the template orientation are of higher importance and no geometry HB control is observed for longer X…H bonds, X = O, N.

Although there are differences in the HBs between the template and dense or open ALPOs, similarities between the atomic multipole moments (AMMs) were observed between these calcined sieves. The approximation of the AMMs in terms of the cumulative coordinate (CC) scheme [11] showed close correlations between the same O types determined by their interactions with the nearest neighbors. Separate approximations of the AMMs were required for three O types, *i.e.*, HB oxygen atoms, non-HB oxygen atoms, and the oxygens of the Al-O bonds which are elongated up to 1.86 Å. Accurate approximations for the Al hexadecapole moment at the AlO_6 position were obtained in both as-synthesized $AlPO_4$-14 and $AlPO_4$-15 forms. This is in agreement with the capabilities of the CC method observed earlier; it provides accurate approximations of the most important AMMs for the electrostatic properties even if they are of the highest orders [11].

Bond critical points (CPs) of the O…H and Al-O bonds were characterized with the NEWPROP code using the experimental electron density (ED) determined by XRD and compared to the CPs obtained, with the TOPOND code, from the ED calculated at different levels of theory. Both the PHF and periodic DFT methods showed an exaggerated ED slope with the O…H distance as compared to the experimental ED dependence, but the difference between the theoretical and experimental ED does not exceed 20 % within the O…H range of 1.8 - 2.2 Å. The ED at the CP positions of the Al-O bonds correlates with the Al-O length for all AlO_n (n = 4-6) types, which supports the proposition of a slight variation of the electronic structure of the framework Al atoms while changing the Al coordination.

ACKNOWLEDGEMENTS

AVL and DPV wish to thank the FUNDP for the use of the Namur Scientific Computing Facility (SCF) Centre. They are grateful for the partial support of the Interuniversity Research Program on "Quantum Size Effects in Nanostructural Materials" (PAI/IUAP 5/01). The authors thank Dr. R.W. Broach for the corrected coordinates of the $AlPO_4$-14 sieve.

REFERENCES

1. Bennet, J.M., Dytrych, W.J., Pluth, J.J., Richardson Jr., J.W., Smith, J.V., Zeolites, 6 (1986), 349-359.
2. Wilson, S.T., Lock, B.M., Mesina, C.A., Cannon, T.R., Flanigen, E.M., Amer. Chem. Soc. Symp. Ser. 218 (1992), 79.
3. Broach, R.W., Wilson, S.T., Kirchner, R.M. Proc. 12th Intern. Zeolite Conf., 1999, 1715-1722.
4. Cox, P.A., Stevens, A.P., Banting, L., Gorman, A.M., Stud. Surf. Sci. Cat., 84 (1994), Part C, 2115-2122.
5. O'Malley, P.J., *ibid.,* 2163-2170.
6. Corma, A., Sastre, G., Viruela, P., *ibid.*, 2171-2178.
7. Corà, F., Catlow, C.R.A., D'Ercole, A. J. Mol. Cat. A, 166 (2001), 87-99.
8. Sastre, G., Lewis, D.W., J. Chem. Soc. Faraday Trans., 94 (1998), 3049-3058.
9. Jeanvoine, Y., Ángyán, J.G., Kresse, G., Hafner, J. J. Phys. Chem. B, 102 (1998), 5573-5580.
10. Jeanvoine, Y., Ángyán, J.G., Kresse, G., Hafner, J. J. Phys. Chem. B, 102 (1998), 7307-7310.
11. Larin, A.V., Vercauteren, D.P., Int. J. Quant. Chem., 83 (2001), 70-85.
12. Larin, A.V., Vercauteren, D.P. J. Mol. Cat. A, 166 (2001), 73-85.
13. Saunders, V.R., Dovesi, R., Roetti, C., Causà, M., Harrison, N.M., Orlando, R., Zicovich-Wilson, C.M. Crystal98 1.0, User's Manual, Torino, 1999.
14. Gale, J.D. GULP 1.3, Royal Institution/Imperial Colledge, UK, 1992/1994.
15. Schroder, K.P., Sauer, J., Leslie, M., Catlow, C.R.A., Thomas, J.M., Chem. Phys. Lett., 188 (1992), 320-325.
16. Gale, J.D., Henson, N.J., J. Chem. Soc. Faraday Trans., 90 (1994), 3175-3181.
17. Cerius 2, User's Guide, Version 4.0.0; MSI, San Diego (1997).
18. Broach, R.W., personal communication.
19. Aubert, E., Porcher, F., Souhassou, M., Lecomte, C., Acta Cryst., B59 (2003), 687-700.
20. Bader, R.F.W. Atoms in Molecules: A Quantum Theory; Clarendon Press: Oxford, 1995.
21. Gatti, C. TOPOND-96: an electron density topological program for systems periodic in N (N = 0-3) dimensions, User's Manual, CNR-CSRSRC, Milano, 1996.
22. Souhassou M., Blessing R.H., J. Appl. Cryst., 32 (1999), 210-217.
23. Gaussian 98, Revision A.7, Frisch, M.J., *et al.* Gaussian, Inc., Pittsburgh PA, 1998.
24. Xantheas, S.S., Dunning Jr., T.H., J. Chem. Phys., 99 (1993), 8774-8792.
25. Ibers, J.A., Stevenson, D.P., J. Chem. Phys., 28 (1958), 929-940.
26. Teunissen, E.H., Jansen, A.P.J., van Santen, R.A., J. Phys. Chem., 99 (1995), 1837-1879.
27. Greatbanks, S.P., Sherwood, P., Hillier, I.H., Hall, R.J., Burton, N.A., Gould, I.R., Chem. Phys. Lett., 234 (1995), 367-372.
28. Chase, M.W., Jr., Davies, C.A., Downey, J.R., Jr., Frurip, D.J., McDonald, R.A., Syverud, A.N. Janaf Thermochemical Tables, J. Phys. Chem. Ref. Data, 14 (1985), Suppl 1.
29. Cox, P.A., Casci, J.L., Stevens, A.P., Faraday Discuss., 106 (1997), 473-487.
30. Larin, A.V., Trubnikov, D.N., Vercauteren, D.P., Chem. Phys. Lett., submitted, VS-03-0028.
31. Pluth, J.J., Smith, J.V., Bennet, J.M., Cohen, J.P., Acta Cryst., C40 (1984), 2008-2011.